Title

Microcontact printing of choline oxidase using a polycation-functionalized zwitterionic polymer as enzyme immobilization matrix.

Journal

Analyst, 148(23)

Authors

Zhao, Ming
Cao, Yan
Huang, I-Wen
et al.

Publication Date

2023-11-20

DOI

10.1039/d3an01263h

Peer reviewed

HHS Public Access

Author manuscript

Analyst. Author manuscript; available in PMC 2024 November 20.

Published in final edited form as:

Analyst. ; 148(23): 5949–5956. doi:10.1039/d3an01263h.

Microcontact Printing of Choline Oxidase using a Polycation-Functionalized Zwitterionic Polymer as Enzyme Immobilization Matrix

Ming Zhao[†,‡],

Yan Cao[‡],

I-wen Huang[‡],

Harold G. Monbouquette

Chemical and Biomolecular Engineering Department, University of California, Los Angeles, Los Angeles, CA 90095, USA.

Abstract

Highly sensitive and selective choline microbiosensors were constructed by microcontact printing (μCP) of choline oxidase (ChOx) in a crosslinked, polyamine-functionalized zwitterionic polymer matrix on microelectrode arrays (MEAs). μCP has emerged as a potential means to create implantable, multiplexed sensor microprobes, which requires the targeted deposition of different sensor materials to specific microelectrode sites on a MEA. However, the less than sufficient enzyme loading and inadequate spatial resolution achieved with current μCP approaches has limited adoption of the method for electroenzymatic microsensors. A novel polymer, poly(2-methacryloyloxyethyl phosphorylcholine)-*g*-poly(allylamine hydrochloride) (PMPC-*g*-PAH), has been developed to address this challenge. PMPC-*g*-PAH contributes to a higher viscosity "ink" that enables thicker immobilized ChOx deposits of high spatial resolution while also providing a hydrophilic, biocompatible microenvironment for the enzyme. Electroenzymatic choline microbiosensors with sensitivity of 639 ± 96 nA μM^{-1} cm^{-2} (pH 7.4; $n = 4$) were constructed that also are selective against both ascorbic acid and dopamine, which are potential electroactive interfering compounds in the mammalian brain. The high sensitivities achieved can lead to smaller MEA microprobes that minimize tissue damage and make possible the monitoring of multiple neurochemicals simultaneously *in vivo* with high spatial resolution.

Graphical Abstract

hmonbouq@ucla.edu .

[†]Current address: Department of Pharmaceutical Chemistry, School of Pharmacy, University of Kansas, 2095 Constant Avenue, Lawrence, Kansas 66047.

[‡]These authors contributed equally to this work.

Author Contributions

M. Zhao, I-w. Huang and Y. Cao: data curation, formal analysis, investigation, methodology, validation, visualization, writing—original draft, writing—review & editing. H. G. Monbouquette: formal analysis, funding acquisition, methodology, project administration, resources, supervision, validation, visualization, writing—review & editing.

Conflicts of interest

There are no conflicts to declare.

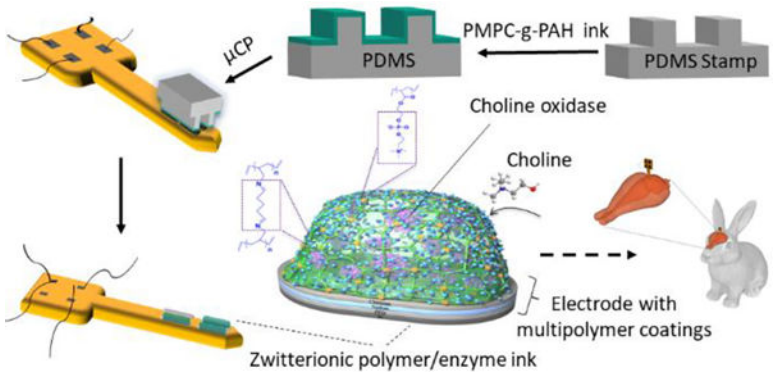

Microcontact printing of choline oxidase on an implantable, microelectrode array probe using an "ink" based on the novel polymer, PMPC-g-PAH, to create high-performance choline biosensors

Introduction

The capability to monitor simultaneously multiple neurochemicals *in vivo* in near-real-time with high selectivity and spatial resolution has triggered interest from neuroscientists, as behaviors and physiological disorders are controlled by neuronal networks influenced by the complex interplay among various neurotransmitters.[1, 2] While conventional microdialysis enables the monitoring of multiple analytes simultaneously and has provided important insight into the regulation of neurotransmissions, this technique is constrained by its generally low temporal resolution in the range of minutes.[3–6] In contrast, electrochemical techniques based on implantable microprobes with an array of electroenzymatic sensing sites offers a means for multianalyte sensing at high temporal as well as spatial resolution and has developed rapidly into a robust analytical technique for neurotransmitters over the past few years.[7–11] Electroenzymatic sensors typically rely on specific oxidase enzymes to catalyze oxidations of the target analyte to produce hydrogen peroxide (H_2O_2) that is oxidized or reduced at an underlying electrode at moderate potential to give a current signal. Development of microelectrode array (MEA) microprobes for multiple neurotransmitter detection consequently requires a method to selectively deposit multiple different enzymes onto specific microelectrode sites of a MEA microprobe.

Enzyme deposition and immobilization on microelectrode surfaces is achieved most commonly by manually loading a mixture of enzyme, bovine serum albumin (BSA), and glutaraldehyde (GAH) as crosslinker on the electrode surface.[11–13] However, the manual approach becomes problematic when the MEA feature size is in the micrometer range. In previous work, we demonstrated the use of microcontact printing (μCP) for creation of multianalyte sensing microprobes by patterning two different enzyme/BSA mixtures onto selected, distinct sites on a MEA and subsequent crosslinking with GAH vapor.[14, 15] Although this accomplishment demonstrates the potential of MEAs for recordings of multiple neurochemicals simultaneously *in vivo* with high spatiotemporal resolution, the use of enzyme/BSA mixtures in aqueous solution as the "ink" has important disadvantages. Since the BSA protein behaves as a globular particle in solution that contributes little to the viscosity of the "ink", imprinted enzyme patterns tend to be so thin that low sensitivity

results or problematic surface spreading and low spatial-resolution deposits occur when higher enzyme loading is attempted. For the application described in this work, excessive spreading of “ink” deposits is highly undesirable as it can lead to contamination of adjacent microelectrodes less than 100 μm away resulting in sensor crosstalk. As these problems are inherently related to ink properties, there has been a need for a new formulation that provides high adhesion to substrate and stronger intermolecular forces for higher viscosity, yet surface functionality similar to BSA to enable enzyme immobilization through covalent crosslinking.

While great strides have been made in modifying “ink” properties to achieve high resolution patterns, the focus has been on creating very thinly layered patterns of molecules, including proteins, on substrates via microstamping.[16–18] In this report, we describe design of a novel graft polymer, poly(2-methacryloyloxyethyl phosphorylcholine)-*g*-poly(allylamine hydrochloride) (PMPC-*g*-PAH) (Fig. 1), which serves as an alternative enzyme immobilization matrix to BSA that enhances the capability and efficiency of enzyme transfer to microelectrode surfaces via μCP. The zwitterionic polyphosphorylcholine moieties of the graft polymer, MPC, serve to enhance surface hydrophilicity and biocompatibility,[19, 20] while the free amine groups of the PAH backbone provide functional groups for crosslinking with GAH vapor thereby entrapping enzyme on the microelectrode surface. The polymer itself provides the added benefit of increased solution viscosity so as to curtail undesirable ink spreading beyond the microelectrode targeted with the microstamp. The minimization of ink surface spreading also enables longer stamp alignment times and enhanced control of enzyme loading for better sensor performance, while the PMPC-g-PAH polymer also minimizes the immune response thereby potentially improving long-term stability *in vivo*.[21]

Experimental

Materials

Nafion (5 wt% in lower aliphatic alcohols and 15–20% water), *m*-phenylenediamine (PD), BSA lyophilized powder, choline oxidase (ChOx) from *Alcaligenes* sp., choline chloride (Ch), L-ascorbic acid (AA), 3-hydroxytyramine (dopamine, DA), chitosan (from crab shells, minimum 85% deacetylated), GAH (25% in water), sodium phosphate dibasic, sodium chloride, hydrochloric acid (HCl, 36.5–38%), H_2O_2 (30 wt% aqueous solution), polyallylamine hydrochloride (PAH, MW 17,500), 2-methacryloyloxyethyl phosphorylcholine (MPC), dimethyl sulfoxide (DMSO), 4-cyano-4-(phenylcarbonothioylthio)pentanoic acid, and poly(*N*-(3-aminopropyl)methacrylamide) were purchased from Sigma-Aldrich (St. Louis, MO). 1-Ethyl-3-(−3-dimethylaminopropyl) carbodiimide hydrochloride (EDC), *N*-hydroxysuccinimide (NHS), 2,2’-azobis[2-(2-imidazolin-2-yl)propane] dihydrochloride (VA-044), and isopropyl alcohol (IPA) were purchased from Thermo Fisher Scientific (Waltham, MA). Solvents were used as received. Ag/AgCl glass-bodied reference electrodes with NaCl electrolyte (3M) and 0.5-mm-diameter platinum (Pt) wire auxiliary electrodes were obtained from BASi (West Lafayette, IN). Sodium phosphate buffer (PBS, pH 7.4) used for sensor calibration was composed of 50 mM sodium phosphate dibasic and 100 mM sodium chloride. Four-inch silicon

(Si) wafers (p-type boron doped; thickness 150 μm) were purchased from Silicon Valley Microelectronics (Santa Clara, CA). SU-8 2075 and SU-8 developer were obtained from MicroChem (Westborough, MA). The Sylgard® 184 silicone elastomer kit was purchased from Dow Corning (Auburn, MI).

Instrumentation

Electrochemical preparations and *in vitro* calibrations were performed using a Versatile Multichannel Potentiostat (VMP3, Bio-Logic) equipped with the 'p' low-current option and low-current N stat box. A standard three-electrode system consisting of a separate Pt-wire as counter electrode, a separate Ag/AgCl reference electrode and modified Pt microelectrode sites on our MEA microprobe as the working electrodes was used in a Faraday cage. The film thicknesses on microelectrodes were measured using a SEM (Nova 600 SEM/FIB system).

Synthesis of PMPC conjugated PAH via RAFT polymerization (PMPC-g-PAH)

The PAH macroCTA was synthesized by conjugating the chain transfer agent (CTA) to the amino groups of PAH. Briefly, 3 mg of 4-cyano-4-(phenylcarbonothioylthio) pentanoic acid was dissolved in 400 μL DMSO. The DMSO solution was mixed with 10.5 mg EDC and 2.5 mg NHS in 50 μL 2-(*N*-morpholino)ethanesulfonic acid (MES) buffer (pH 5.0), followed by incubation at 4 °C for 1 h. Next, 20 mg of PAH in 100 μL of MES buffer was added. The mixture was stirred at room temperature for 24 h. Afterwards, the reaction mixture was dialyzed against acetate buffer (pH 5.0) for 4 h to remove EDC, NHS, DMSO and unreacted CTA. The conjugation ratio was determined from UV-vis spectra. The final product was obtained by freeze-drying as a pink solid.

The PMPC-*g*-PAH graft polymer was synthesized via reversible addition-fragmentation chain-transfer (RAFT) polymerization (Fig. 1). First, 10 mg of PAH macroCTA (0.0054 mmol), 80 mg MPC (0.27 mmol), and 8.7 mg VA-044 (0.027 mmol) were dissolved in 500 μL of acetate buffer at pH 5.0 and added to a Schlenk flask. The mixture was deoxygenated through three, freeze-pump-thaw processes. Next, the flask was placed in a water bath at 25 °C and stirred for 6 h. The polymerization was stopped by immersing the flask in liquid nitrogen. Finally, the reaction solution was dialyzed against DI water to remove the unreacted initiator and monomer. The final product was obtained by freeze drying. The successful synthesis of PMPC-*g*-PAH was verified from the H^1NMR spectrum (Fig. 2), which showed each side chain contains about 50 MPC units per pendant PMPC chain and the average molecular weight was approximately 16.6K per polymer chain.

Fabrication of mold and polydimethylsiloxane (PDMS) stamps

SU-8 2075 was spin-coated at 2000 rpm for 30 seconds on a four-inch Si wafer to give a ~100 μm thick layer. Next soft bakes were conducted at 65 °C for 5 min and then at 95 °C for 40 min followed by 27 s of UV exposure using a Karl Suss MA6 contact aligner with 8 mJ/cm^2 sec setting through a chromium mask for microstamp mold patterning (total exposure 216 mJ/cm^2 at 365 nm). After UV exposure, the spin-coated SU-8 layer was baked once again at 65 °C for 5 min and then at 95 °C for 10 min. The mold pattern was

developed in SU-8 developer for 20 min, followed by IPA cleaning and drying in air at room temperature.

PDMS microstamps were fabricated using the Sylgard® 184 silicone elastomer kit. Six grams of monomer were mixed with 0.6 g of curing agent (10: 1; monomer: curing agent) and then centrifuged at 15,000 rpm for 5 min to remove air bubbles and degassed under vacuum. After pouring into the SU-8 mold, the PDMS was degassed under vacuum to remove any remaining air bubbles followed by curing at 60 °C for 4 h. The molded PDMS subsequently was detached from the SU-8 mold and cut into 1 cm × 1 cm pieces. The size of the microstamp surface (50 μm × 160 μm) was designed to be slightly larger than the size of a microelectrode to ensure complete coverage. The PDMS stamps were cleaned in 7.5% H_2O_2 and sonicated before each use.

Sensor preparation

The silicon-based MEA probes were manufactured from 4-in, 150-μm-thick Si wafers in-house using previously described microelectromechanical system (MEMS) techniques.[11] The processes included the physical vapor deposition of Pt as electrode material, and the chemical vapor deposition of silicon oxide/nitride as insulation. Shaping was done by deep reactive ion etching from the front side. Each probe was 150 μm thick, 140 μm wide and 9 mm long, with four Pt recording sites (40 μm × 150 μm) at the tip arranged in pairs separated by 40 μm (Fig. 3).

The choline sensor design is shown in Fig. 4. A polyphenylenediamine (PPD) film first was electrodeposited on the Pt microelectrodes from a 5 mM PD solution in PBS (0.1 M) by holding the voltage constant at 0.85 V vs. Ag/AgCl for 20 mins. Afterward, a Nafion layer was dip-coated from a 2% Nafion solution (diluted from stock with 4:1 IPA:water and annealed at 115 °C for 20 min). Next, a 0.1% w/v aqueous chitosan solution for subsequent chitosan deposition was prepared by mixing chitosan into water and adjusting the pH to 3 using HCl (0.1 M) followed by stirring for over 48 h to ensure complete dissolution of chitosan flakes. Subsequently, the solution was filtered using a 0.2 μm syringe filter, and the pH was adjusted to 5 with NaOH solution (0.5 M). The MEA probe coated with PPD and Nafion then was immersed in the aqueous chitosan preparation, and a constant potential of −0.7 V vs. Ag/AgCl was applied at the Pt microelectrode surfaces for 1 min, and repeated twice more for 1 min each, to electrodeposit the chitosan film.[22, 23]

The enzyme “ink” was prepared by mixing 4 μL ChOx (0.5 U/μL) with either 1 μL PMPC-*g*-PAH polymer solution (20 mg/ml) or 2 μL BSA solution (60 mg/ml). A droplet (~3 μL) of the prepared enzyme “ink” was deposited on the PDMS microstamp and after ~20 mins in air at room temperature, the inked stamp was aligned carefully to the target microelectrode surface under a microscope fitted with a custom-built, manually adjustable stage to position the stamp.[14] (Note that a substantially longer drying time may be necessary in a very humid environment, while a shorter drying time may be appropriate at very low ambient humidity.) Deposition on the desired microelectrode surface was performed by adjusting the stage to achieve gentle contact of the PDMS stamp coated with viscous enzyme “ink” with the electrode surface for a few seconds. A wet enzyme layer remained after removal of the

PDMS stamp as illustrated in Fig. 5.[14] Finally, the printed enzyme layer was exposed to vapor from a 5% GAH aqueous solution for 1 min to effect crosslinking.

Sensor calibration

Constant potential amperometric measurements were conducted in stirred PBS buffer at 0.7 V vs. Ag/AgCl and ambient temperature. The sensors were permitted to equilibrate in PBS buffer for approximately 30 mins before adding analytes. Solutions of AA, DA, Ch or H_2O_2 were added individually to the stirred buffer solution to give final concentrations of 250 μM AA, 10 μM DA, 20–60 μM Ch and 20 μM H_2O_2 to assess sensitivity and selectivity. The sensitivity was calculated from the slope of the linear portion of the calibration curve divided by the area of the electrode.

Results and discussion

BSA-ChOx ink

Unlike many applications of μCP for deposition of monolayer-thick patterns of protein, the goal here was to deposit a ~4–5-μm-thick film corresponding to many equivalent enzyme layers on a well-defined microelectrode substrate in order to give optimal sensor performance.[24] The printing of a thick pattern with micron-scale, lateral spatial resolution is challenging; as it requires a good combination of surface wettability of the ink and ink viscosity (Fig. 6), since the chitosan film on the microelectrodes presents a hydrophilic surface for a water-based ink to wet and spread. If a conventional enzyme ink composed of ChOx and BSA in water is permitted to dry for ~35–45 mins on the PDMS stamp before transfer in an effort to increase ink viscosity and reduce spread, the resulting pattern was limited to the microelectrode surface but was too thin (in the few hundred nm range) and showed incomplete coverage (Fig. 6a). In contrast, if the ChOx/BSA ink is permitted to dry <10 mins on the PDMS surface before stamping, this wet ink also was not preferred as it spread laterally, well beyond the edges of the microelectrode (Fig. 6b). Adequate spatial resolution was achieved after pre-drying the ink on the stamp for 15–20 mins, which presumably resulted in an ink state with sufficiently reduced water content (Fig. 6c). However, the deposit was only 2-μm-thick, which is less than half optimal. In our prior work with the BSA-based ink, at least two stamping cycles were required to obtain a high performance choline sensor.[14] Also, subsequent unacceptable surface spreading was observed during the crosslinking step with humid GAH vapor (Fig. 7). It was hypothesized that these problems were related to the inherent ink properties, as both BSA and ChOx behave as globular particles that provide relatively weak intermolecular forces within the ink thereby resulting in ink viscosity that is too low to control spreading on a chitosan-coated microelectrode surface. Finally, the narrow drying time window during which nearly acceptable stamping can be achieved made manual alignment of the microstamp and the targeted microelectrode a challenging process. These issues prompted formulation of alternative ChOx-containing inks that could be used to deposit sufficiently thick enzyme layers with good spatial resolution that also could be crosslinked effectively.

PMPC-*g*-PAH-ChOx ink

It is known that the physical properties of the polymer incorporated in enzyme ink are particularly important in determining enzyme transfer efficiency during μCP.[25] The key to enable high enzyme loading without surface spreading on a hydrophilic surface is to add a hydrophilic polymer with sufficiently strong intermolecular interactions, due to for example, entanglements, hydrogen bonding and van der Waals forces. Initially, experiments were conducted with poly(*N*-(3-aminopropyl)methacrylamide) (PAPM), a polymer of easily tuned length through free-radical polymerization that also provides free amine-groups for GAH crosslinking (data not shown). Although higher molecular weight PAPM provided better control of ink spreading, the preparation was too viscous to provide the flexibility needed to control the thickness of printed patterns. However, these initial PAPM trials provided valuable insight into the influence of polymer characteristics on enzyme μCP and led to the choice of commercially available PAH (MW = 17,500 g/mol) as a promising alternative for future work due to its well-defined structure, convenient chemistry for modifications, and low price.

To further enhance PAH-based ink hydrophilicity and to improve biocompatibility of printed enzyme patterns, the zwitterionic monomer, MPC, was conjugated to PAH to synthesize the polymer, PMPC-*g*-PAH. Zwitterionic polymers have been used widely as ultralow fouling coatings on biomedical devices due to their super hydrophilic nature that forms a surrounding shell of water molecules to inhibit protein adsorption.[20, 26] In addition, it is known that water-soluble enzymes tend to keep their active conformation in more hydrophilic environments. The hydrophilicity of PMPC-*g*-PAH was assessed and confirmed by measuring the contact angle on a hydrophobic PDMS stamp that showed a large angle of over 90° (Fig. 8). Therefore, PMPC-g-PAH showed clear promise as a key component of an enzyme ink formulation.

Subsequent tests were conducted to assess the performance of the PMPC-*g*-PAH-based ink for μCP of ChOx onto coated Pt microelectrodes. As shown in Fig 9, the thickness of the printed ChOx layer with PMPC-g-PAH-based ink was measured at ~4 μm without observable surface spreading after exposure to GAH/water vapor. This layer thickness was ~2-fold thicker than that obtained with the BSA-ChOx and close to the predicted optimal thickness for electroenzymatic choline sensors.[24] Moreover, use of the PMPC-g-PAH-ChOx ink greatly improved the μCP success rate by enabling a much longer stamp alignment time with gentle contact between stamp and microprobe. This could be attributed to the stronger hydrogen bonding of water to the zwitterionic PMPC side chains, which slow the water evaporation rate from the ink.

Stamped choline microsensor performance

To demonstrate that enzyme function was retained after μCP and crosslinking, all microsensors were tested with choline in solution at 0 to 60 μM and at a constant operating potential of 0.7 V vs. Ag/AgCl (Fig. 10a). The choline sensor selectivity was also tested against two common electrooxidizable interferents, AA and DA at 250 μM and 10 μM respectively, which are found in brain extracellular fluid at 200–400 μM for AA and 10 nM to 1 μM for DA.[27, 28] As expected, the data showed an increase in sensitivity with increased

thickness of the immobilized ChOx deposit up to a maximum of ~4 μm. Compared to our previous work where BSA-ChOx ink was used to create a thin immobilized ChOx deposit (estimated at <1 μm) that resulted in a sensitivity of 286 ± 63 nA μM^{-1} cm^{-2},[14] a ~1.5-fold improvement in Ch sensitivity was achieved simply by creating a thicker BSA-ChOx deposit here of ~2 μm (with some compromise in spatial resolution) that resulted in a sensitivity of 444 ± 133 nA μM^{-1} cm^{-2} (n = 5) (Fig. 10b). A further increase in ChOx loading corresponding to a high spatial resolution deposit of ~4 μm in thickness when PMPC-*g*-PAH was used as enzyme matrix, led to another 1.5-fold improvement in sensitivity to 639 ± 96 nA μM^{-1} cm^{-2} (n = 4). Importantly, these highly sensitive devices showed no discernible response to AA or DA (Fig. 10a). Also, as these improvements in sensitivity were achieved without sacrificing background noise, the limit of detection (at signal-to-noise ratio of 3) of printed PMPC-*g*-PAH-ChOx sensors relative to printed BSA-ChOx sensors was also improved, 0.31 ± 0.06 μM (n = 4) versus 0.45 ± 0.17 μM (n = 5), respectively (Fig. 10c). The response time was estimated to be around 0.57 s ± 0.39 s (n = 9) despite thicker immobilized ChOx deposits. The high sensitivity obtained with PMPC-*g*-PAH-ChOx stamped microsensors exceeds that of most other published choline sensors, including those that employed manual, non-stamping enzyme deposition methods in their construction and is statistically the same as the highest recorded sensitivity that was achieved by manually spreading and crosslinking 12–15 layers of BSA-ChOx solution on a microelectrode in order to achieve a ~4-μm-thick deposit.[14, 24, 29–33]

Apparent immobilized ChOx kinetics

The apparent Michaelis-Menten parameters, I_{max} and K_m^{app} (Eq. 1) were estimated for the choline biosensors to provide insight into factors affecting the sensitivity measurements presented above. Here, the concentration of co-substrate O_2 is assumed constant, and K_m^{app} is defined as the Ch concentration at half the corresponding I_{max}.

$$I = \frac{I_{max}[\mathrm{Ch}]}{K_m^{app} + [\mathrm{Ch}]} \quad (1)$$

As shown in Fig. 11, a ~1.5-fold increase in I_{max} achieved with PMPC-g-PAH-ChOx stamped microsensors compared to those stamped with BSA-ChOx indicated greater enzyme activity and/or improved mass transfer characteristics of the PMPC-g-PAH-ChOx layer transferred onto the electrode surface.[34] However, one would expect a greater K_m^{app} value with the 2-fold thicker PMPC-*g*-PAH-ChOx layer, yet it was essentially the same as that for the BSA-ChOx biosensor, 110 ± 18 μM (n = 4) versus 101 ± 27 μM (n = 5), respectively. Zwitterionic polymers such as PMPC have the unique property of retaining or improving binding affinity through enhanced protein-substrate hydrophobic interactions.[35] Unlike BSA (pI: 4.7) that provides a net negatively charged matrix at neutral pH, the PMPC-g-PAH polymer is positively charged, thereby counterbalancing the net negatively charged ChOx (pI: ~4.5) and enabling more effective loading of the enzyme on the microelectrode.[36] This possibility is consistent with a report describing a large decrease in K_m^{app} when Pt electrodes are pre-coated with a polycationic species.[37] The positively charged PMPC-g-PAH polymer

also may improve partitioning of negatively charged Ch into the immobilized enzyme layer resulting in a locally higher concentration in the layer as opposed to the solution. In addition, choline and/or H_2O_2 effective diffusivity in the PMPC-g-PAH-ChOx layer may be improved, a possibility that would require further experimentation to determine the mass transfer characteristics of the immobilized enzyme layer.[38] Nevertheless, these results demonstrate improved choline sensor performance using the GAH crosslinked PMPC-g-PAH matrix for the immobilized enzyme layer rather than the conventional immobilization medium based on crosslinked BSA.

Conclusions

The PMPC-g-PAH polymer has proven to be a far more effective μCP matrix than BSA both for deposition of thicker immobilized ChOx layers on microelectrodes with high spatial resolution and for creation of highly sensitive choline biosensors. Choline biosensors created with the PMPC-g-PAH "ink" exhibited among the highest reported sensitivities, 639 ± 96 nA μM^{-1} cm^{-2} (n = 4); a sub-second response time; and a very low limit of detection, 0.31 ± 0.06 μM (n = 4). Apparent biosensor kinetic data suggest that ChOx is more active in this new matrix. Further, the use of PMPC-g-PAH greatly improved the μCP success rate by lengthening drying time thereby enabling more careful alignment of the stamp with the target microelectrode. Therefore, μCP with PMPC-g-PAH serving as "ink" and as oxidase immobilization matrix is expected to enable construction of MEA microprobes for simultaneous detection of multiple analytes in close proximity, as well as combined neurochemical monitoring and electrical recordings. The higher sensitivity exhibited with the electroenzymatic sensors also will make possible the shrinking of microelectrode and MEA microprobe size so as to minimize tissue damage. Finally, the use of PMPC-g-PAH has the potential to improve stability *in vivo*, as zwitterionic MPC has been widely reported to minimize the immune response.[17, 21, 22]

Acknowledgements

This research was supported by NIH (R01NS087494).

References

1. Levin ED, in Neurotransmitter Interactions and Cognitive Function, ed. Levin ED, Birkhäuser Basel, Basel, 2006, DOI: 10.1007/978-3-7643-7772-4_1, pp. 1–3.
2. Ou Y, Buchanan AM, Witt CE and Hashemi P, Anal Methods, 2019, 11, 2738–2755. [PubMed: 32724337]
3. Bowser MT and Kennedy RT, Electrophoresis, 2001, 22, 3668–3676. [PubMed: 11699904]
4. Rogers ML, Feuerstein D, Leong CL, Takagaki M, Niu X, Graf R and Boutelle MG, ACS Chem Neurosci, 2013, 4, 799–807. [PubMed: 23574576]
5. Rutherford EC, Pomerleau F, Huettl P, Stromberg I and Gerhardt GA, J Neurochem, 2007, 102, 712–722. [PubMed: 17630982]
6. Yang HY, Thompson AB, McIntosh BJ, Altieri SC and Andrews AM, Acs Chemical Neuroscience, 2013, 4, 790–798. [PubMed: 23614776]
7. Collins AL, Aitken TJ, Huang IW, Shieh C, Greenfield VY, Monbouquette HG, Ostlund SB and Wassum KM, Biol Psychiat, 2019, 86, 388–396. [PubMed: 30955842]
8. Burmeister JJ, Price DA, Pomerleau F, Huettl P, Quintero JE and Gerhardt GA, J Neurosci Methods, 2020, 329, 108435. [PubMed: 31600528]

9. Castagnola E, Robbins EM, Krahe DD, Wu B, Pwint MY, Cao Q and Cui XT, Biosens Bioelectron, 2023, 230, 115242. [PubMed: 36989659]
10. Ledo A, Lourenço CF, Laranjinha J, Gerhardt GA and Barbosa RM, Current Opinion in Electrochemistry, 2018, 12, 129–140.
11. Wassum KM, Tolosa VM, Wang J, Walker E, Monbouquette HG and Maidment NT, Sensors-Basel, 2008, 8, 5023–5036. [PubMed: 19543440]
12. Walker E, Wang J, Hamdi N, Monbouquette HG and Maidment NT, Analyst, 2007, 132, 1107–1111. [PubMed: 17955144]
13. Burmeister JJ and Gerhardt GA, Analytical Chemistry, 2001, 73, 1037–1042. [PubMed: 11289414]
14. Wang B, Koo B, Huang L.-w. and Monbouquette HG, Analyst (Cambridge, U. K.), 2018, 143, 5008–5013.
15. Wang B, Koo B and Monbouquette HG, Electroanal, 2017, 29, 2300–2306.
16. Blinka E, Loeffler K, Hu Y, Gopal A, Hoshino K, Lin K, Liu X, Ferrari M and Zhang JX, Nanotechnology, 2010, 21, 415302. [PubMed: 20834118]
17. Buhl M, Vonhoren B and Ravoo BJ, Bioconjug Chem, 2015, 26, 1017–1020. [PubMed: 26030726]
18. Perl A, Reinhoudt DN and Huskens J, Adv Mater, 2009, 21, 2257–2268.
19. Nakabayashi N and Iwasaki Y, Bio-Medical Materials and Engineering, 2004, 14, 345–354. [PubMed: 15472384]
20. Xie X, Doloff JC, Yesilyurt V, Sadraei A, McGarrigle JJ, Omami M, Veiseh O, Farah S, Isa D, Ghani S, Joshi I, Vegas A, Li J, Wang W, Bader A, Tam HH, Tao J, Chen HJ, Yang B, Williamson KA, Oberholzer J, Langer R and Anderson DG, Nat Biomed Eng, 2018, 2, 894–906. [PubMed: 30931173]
21. Zhao M, Xu D, Wu D, Whittaker JW, Terkeltaub R and Lu Y, Nano Research, 2018, 11, 2682–2688.
22. Wu LQ, Gadre AP, Yi HM, Kastantin MJ, Rubloff GW, Bentley WE, Payne GF and Ghodssi R, Langmuir, 2002, 18, 8620–8625.
23. Tseng TTC, Yao J and Chan WC, Biochem Eng J, 2013, 78, 146–153.
24. Huang I. w., Clay M, Cao Y, Nie J, Guo Y and Monbouquette HG, Analyst, 2021, 146, 1040–1047. [PubMed: 33325460]
25. Shitanda I, Oda K, Loew N, Watanabe H, Itagaki M, Tsujimura S and Zebda A, RSC Advances, 2021, 11, 20550–20556. [PubMed: 35479878]
26. Zhang E and Cao Z, Nat Biomed Eng, 2018, 2, 881–882. [PubMed: 31015726]
27. Neal MJ, Cunningham JR and Matthews KL, Investigative Ophthalmology & Visual Science, 1999, 40, 2983–2987. [PubMed: 10549661]
28. Owesson-White CA, Roitman MF, Sombers LA, Belle AM, Keithley RB, Peele JL, Carelli RM and Wightman RM, J Neurochem, 2012, 121, 252–262. [PubMed: 22296263]
29. Burmeister JJ, Pomerleau F, Huettl P, Gash CR, Wemer CE, Bruno JP and Gerhardt GA, Biosensors & Bioelectronics, 2008, 23, 1382–1389. [PubMed: 18243683]
30. Keihan AH, Sajjadi S, Sheibani N and Moosavi-Movahedi AA, Sensors and Actuators B: Chemical, 2014, 204, 694–703.
31. Zhang H, Yin Y, Wu P and Cai C, Biosens Bioelectron, 2012, 31, 244–250. [PubMed: 22119562]
32. Rahimi P, Ghourchian H and Sajjadi S, Analyst, 2012, 137, 471–475. [PubMed: 22140677]
33. Ricci F, Amine A, Palleschi G and Moscone D, Biosens. Bioelectron, 2003, 18, 165–174. [PubMed: 12485762]
34. O'Neill RD, Rocchitta G, McMahon CP, Serra PA and Lowry JP, TrAC Trends in Analytical Chemistry, 2008, 27, 78–88.
35. Keefe AJ and Jiang S, Nat Chem, 2011, 4, 59–63. [PubMed: 22169873]
36. Ikuta S, Imamura S, Misaki H and Horiuti Y, The Journal of Biochemistry, 1977, 82, 1741–1749. [PubMed: 599154]
37. McMahon CP, Rocchitta G, Serra PA, Kirwan SM, Lowry JP and O'Neill RD, Analyst, 2006, 131, 68–72. [PubMed: 16365665]

38. Huang IW, Clay M, Wang SQ, Guo YW, Nie JJ and Monbouquette HG, Analyst, 2020, 145, 2602–2611. [PubMed: 31998887]

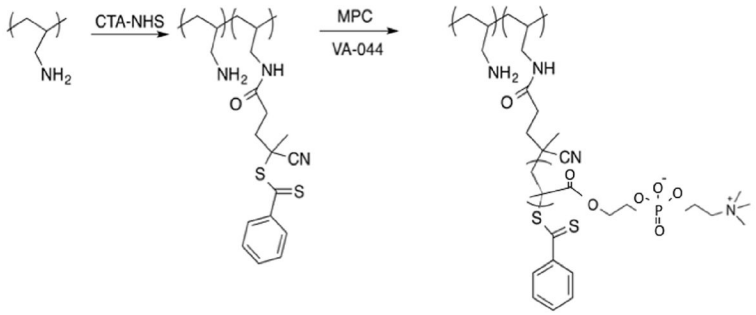

Fig. 1.
Synthesis route to the PAH-*g*-PMPC polymer

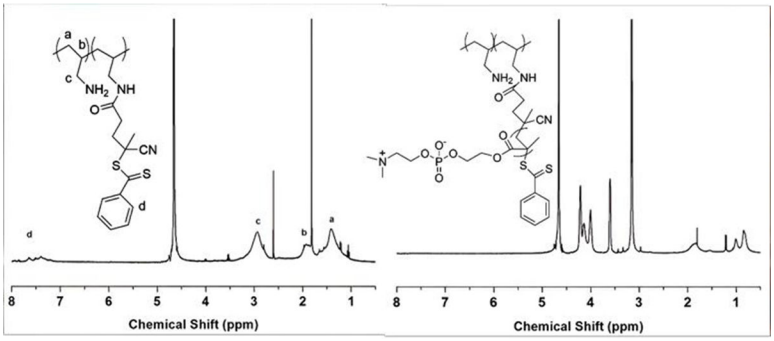

Fig. 2.
Proton NMR of PAH macroCTA and PAH-*g*-PMPC

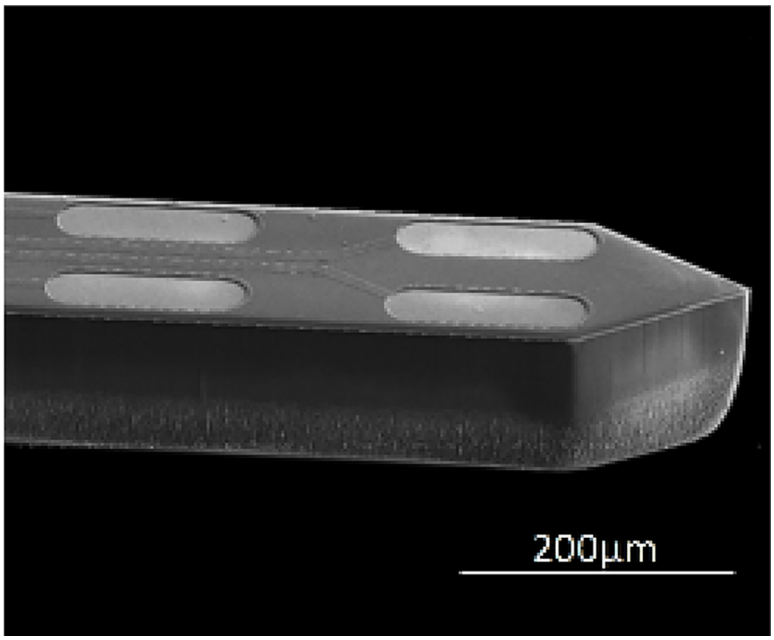

Fig. 3.
Scanning electron microscopy (SEM) image of the MEA probe.

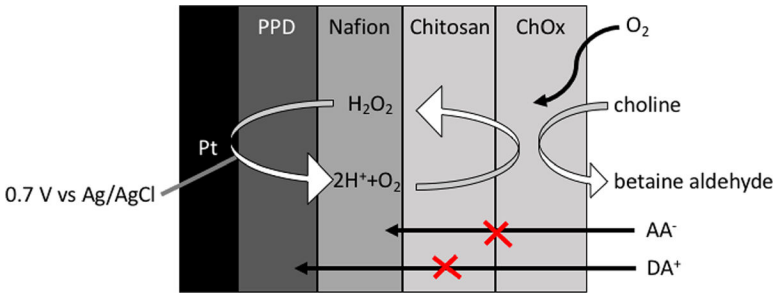

Fig. 4.

Schematic diagram showing the construction of the choline sensors (not to scale) as well as the sensing mechanism. The chitosan layer serves as an adhesive for the immobilized enzyme layer. Nafion acts primarily to reject negatively charged interfering species found in brain extracellular fluid such as ascorbic acid (AA), while the PPD layer acts primarily to reject dopamine (DA). ChOx catalyzes the oxidation of choline to produce H_2O_2, which is electrooxidized at the Pt electrode surface to produce H^+, O_2 and the electrons that give rise to a current signal.

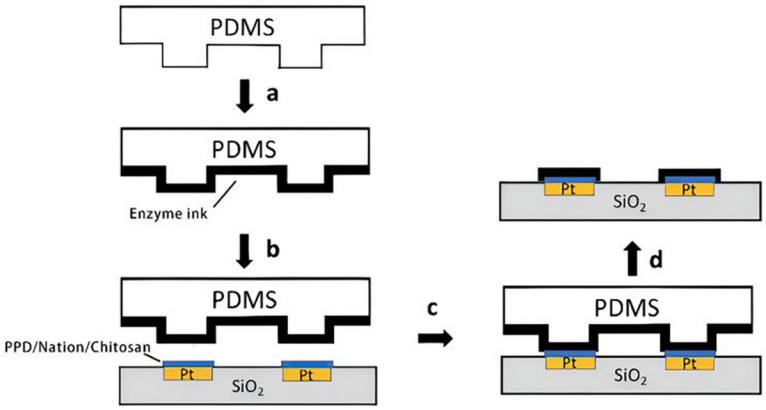

Fig. 5.

Diagram illustrating the enzyme μCP process. (a) The PDMS stamp is wetted with enzyme "ink". (b) The inked stamp is aligned carefully to the target microelectrode surface(s) under a microscope fitted with a custom-built adjustable stage. (c) Gentle pressure is maintained for a few seconds. (d) The stamp is removed leaving an enzyme layer patterned on the targeted microelectrodes of the microprobe (d).

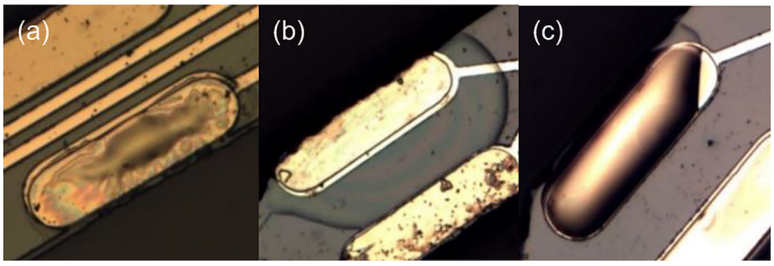

Fig. 6.

Distinct ChOx pattern on chitosan-coated substrate with various wettabilities after PDMS stamping of BSA-ChOx ink. (a) shows insufficient enzyme transfer with ~35–45 mins of incubation time. The PDMS stamp was partially dried, and stamping nearly dry BSA-ChOx ink gave an insufficient enzyme coverage pattern. (b) shows the stamping pattern with less than 10 mins of incubation time. The high mobility of molecules due to excessive wettability caused a severe spreading problem. (c) shows proper wettability with 15 to 20 mins of incubation time. A thick enzyme layer was transferred with an appropriate enzyme coverage pattern.

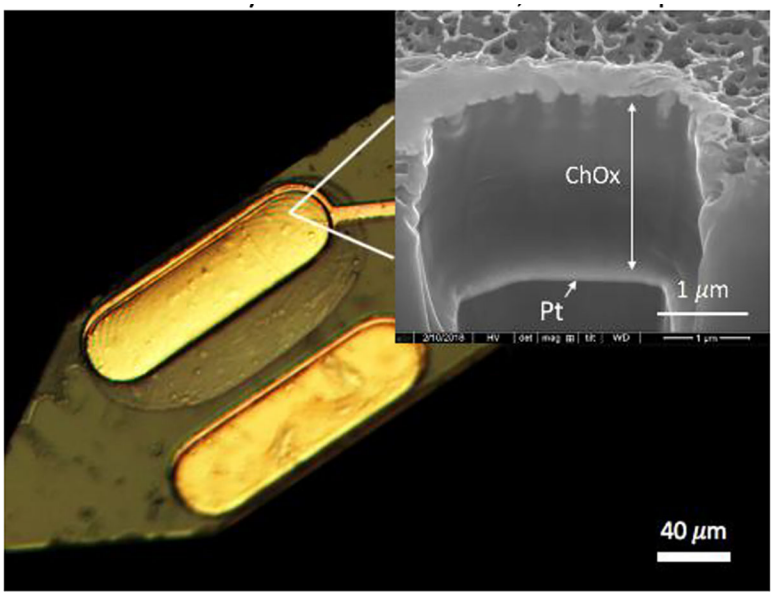

Fig. 7.

Optical microscope image of BSA-ChOx ink pattern stamped on the top microsensor in the micrograph after exposure to humid GAH vapor for crosslinking. The inset shows an SEM image of the ~2-μm-thick deposit cross-section.

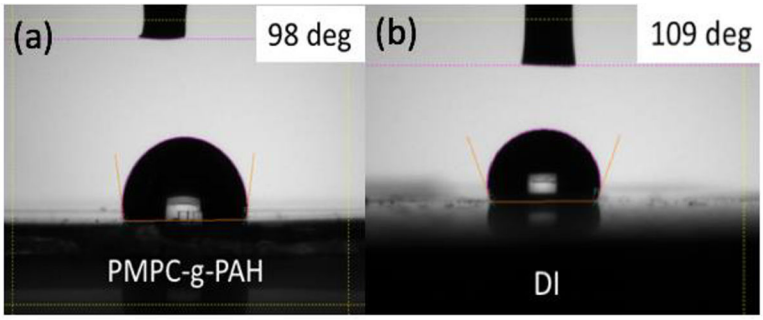

Fig. 8.
Contact angle measurements on PDMS for (a) PMPC-g-PAH (10 mg/ml) and (b) DI water.

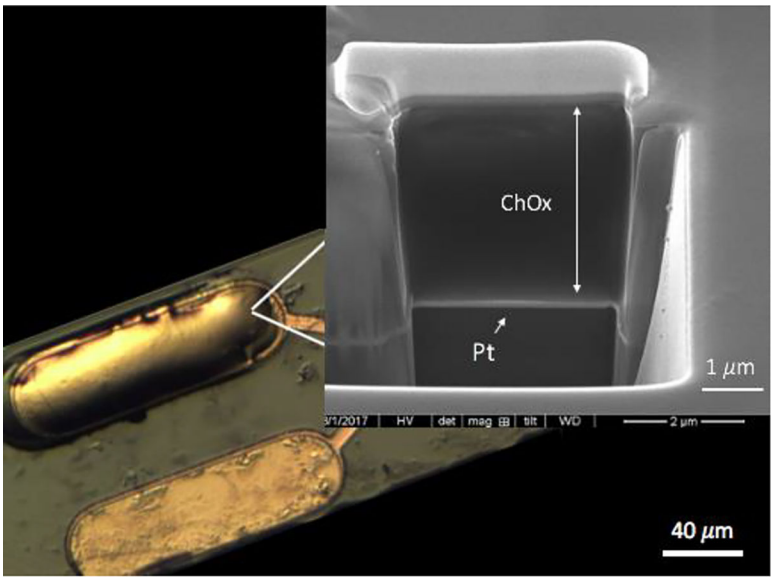

Fig. 9.

Optical microscopy image of PMPC-g-PAH-ChOx ink stamped and GAH crosslinked on a microelectrode (top site). The inset shows the corresponding cross-sectional SEM image.

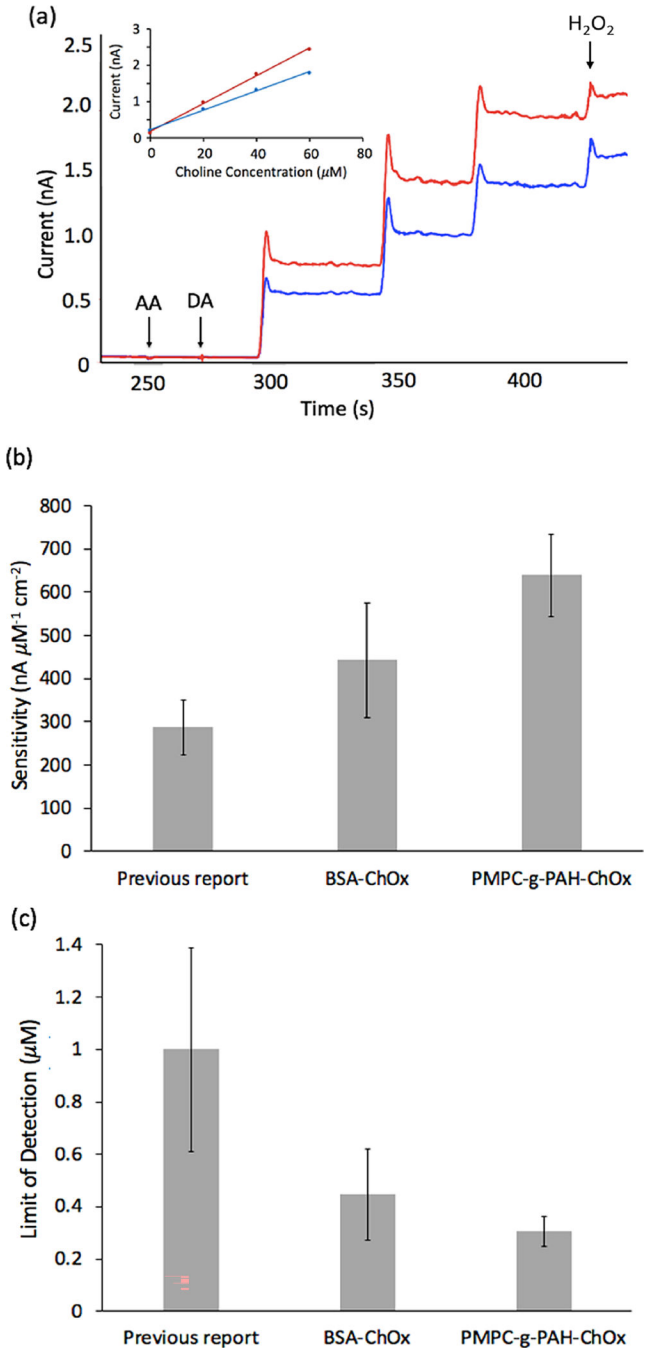

Fig. 10.

Performance of stamped electroenzymatic sensors for choline. (a) Representative current response of stamped BSA-ChOx (blue trace) and stamped PMPC-g-PAH-ChOx (red trace) Ch sensors to interferents, 250 μM AA and 5 μM DA, followed by three 20 μM step increases in Ch concentration and a 20 μM increase in H_2O_2. (b) Ch sensitivities achieved in our previous work with a thin coat of BSA-ChOx ink,[14] this work with a thicker coat of BSA-ChOx ink, and this work with the PMPC-g-PAH-ChOx ink (see text). (c) Ch limits of detection achieved in our previous work with a thin coat of BSA-ChOx ink,[14] this work with

a thicker coat of BSA-ChOx ink, and this work with the PMPC-g-PAH-ChOx ink (see text). Error bars give 95% confident intervals.

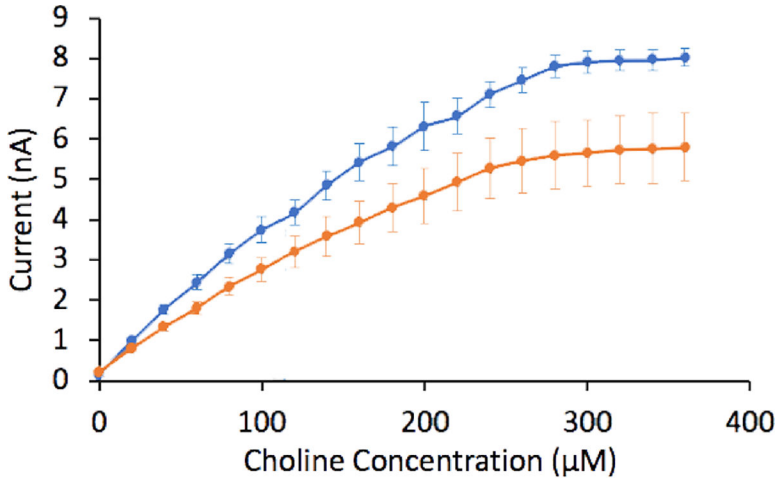

Fig. 11.

Plots of sensor current, *I*, versus choline concentration obtained with sensors stamped with PMPC-g-PAH-ChOx (blue curve: K_m^{app} = 110±18 μM, I_{max} = 7.9±0.6 nA, n = 4) and BSA-ChOx (orange curve: K_m^{app} = 101±27 μM, I_{max} = 5.8±1.7 nA, n = 5) with error bars indicating 95% confident intervals.